C. Micheau and R. Nagarajan. Kinetics and Thermodynamic Modeling of Micellar Autocatalysis. In "Reactions and Synthesis in Surfactant Systems", Ed. J. Texter, Marcel Dekker, New York (2001). Chapter 20. pp. 413–428.

20

Kinetic and Thermodynamic Modeling of Micellar Autocatalysis

JEAN-CLAUDE MICHEAU Laboratoire IMRCP, UMR CNRS 5623, Université Paul Sabatier, Toulouse, France

R. NAGARAJAN The Pennsylvania State University, University Park, Pennsylvania

I. INTRODUCTION

A. Overview

Chemical systems in which molecular aggregates such as micelles are reported to catalyze their own formation have attracted considerable scientific interest. An example is the alkaline hydrolysis of ethyl esters, which displays autocatalytic kinetics. This reaction has been discussed in the literature from the viewpoint of self-replication of molecules in organized compartments such as micelles. The reaction products from the hydrolysis of ethyl alkanoates are ethanol and the corresponding sodium alkanoates. Because the sodium alkanoates are capable of self-assembling into micellar structures, the observed autocatalysis has been attributed to micellar catalysis. However, in spite of their common autocatalytic behaviors, the hydrolysis products from different esters have significantly differing properties. Specifically, the product from the C-4 ester does not form micelles under the reaction conditions, whereas that from the C-8 ester does form micelles. Therefore, autocatalysis cannot be attributed solely to the formation of micelles. More importantly, anionic sodium alkanoate micelles cannot possibly catalyze (in the conventional sense in which catalysis is understood) the hydrolysis reaction involving anionic hydroxyl ions. Therefore, a general kinetic model that can describe the observed autocatalysis is needed in all cases.

Such a model is presented in this chapter. The model is built on a sequence of six events during the hydrolysis of ethyl alkanoates: formation of an ethyl ester–aqueous interface, dissolution of ester in the aqueous phase, hydrolysis of the ester in the aqueous phase, micellization of product sodium alkanoate, solubilization of ester into micelles, and micelle-mediated transport of ester from the organic to the aqueous phase. The dissolution of ester into the aqueous phase is promoted by the salting-in effect of product sodium alkanoate and by the solvent effect of product ethanol. The kinetic model demonstrates that for C-4, taking into account salting-in and solvent effects is sufficient to reproduce the autocatalytic behavior. For C-8, the main step is the micelle-mediated phase transfer of ethyl esters into the aqueous phase. For C-6, in addition to the salting-in and solvent effects and the micelle-mediated ester transport, one has to invoke the possibility that the micelles play yet another role of trapping ester molecules during the initial phase of the reaction without allowing their rapid release into the aqueous phase. Comparison with kinetic experiments performed on different chain lengths of ethyl esters, under different mixing conditions, and for different phase volume ratios has been used to validate the proposed kinetic model of autocatalysis.

B. BLL Reaction

Chemical systems in which molecular aggregates such as micelles have been reported to catalyze their own

formation have attracted considerable scientific interest [1]. A prominent example of such processes is the basic hydrolysis of ethyl octanoate in a biphasic system, which was described originally by Bachmann, Luisi, and Lang [2] and is referred to in this chapter as the BLL reaction. The experimental system they employed is very simple and consists of an organic phase of neat ethyl ester placed above an aqueous alkaline solution. The reacting medium is maintained at 90°C under reflux for many hours, keeping mild stirring conditions so as not to perturb the macroscopic interface between the two immiscible liquids. It is found that there exists a well-defined time period after the start of the reaction during which very little activity takes place. At the end of this quiescent period, the reaction suddenly takes off at a dramatic rate and the overlaying ester is rapidly consumed (Fig. 1).

A qualitative interpretation of the observed kinetic behavior was proposed by the authors (BLL) assuming a micellar catalytic process. The hydrolysis of ester yields ethanol and amphiphilic sodium octanoate, which is known to form anionic micelles in aqueous medium. At the beginning of the reaction, only the ester molecules that are molecularly dissolved in water are available for hydrolysis. Therefore, the amount of product formed is small, reflecting little activity. Correspondingly, the concentration of the product (surfactant) sodium octanoate in the water phase is below the critical value necessary for micellization to start. This initial time period of low activity is observed as the lag time in the kinetic experiments. The surfactant concentration progressively increases with time and eventually reaches the critical micelle concentration (cmc) at which micelles come into existence. Once formed, the micelles can capture large numbers of ester molecules at the interface and carry them into the bulk aqueous phase where hydrolysis occurs, leading to autocatalytic production of the surfactant.

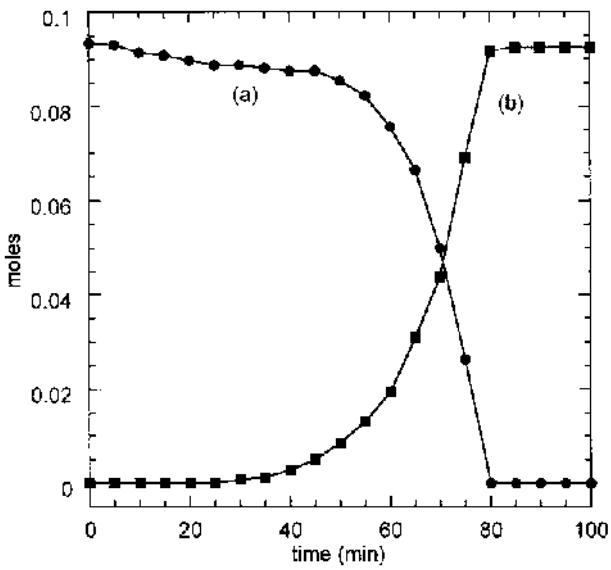

FIG. 1 Kinetics of the biphasic basic hydrolysis of ethyl octanoate performed in a 250-mL round-bottom flask at 90°C by vigorous mixing of 70 mL aqueous 3 M NaOH and 19 mL neat ethyl octanoate with a 25 × 6 mm magnetic bar at 800 rpm. (a) Evolution of ethyl octanoate (total volume of the supernatant organic phase). (b) Evolution of the concentration of the sodium octanoate in the aqueous phase. As in the original BLL reaction, we have observed a quiescent period followed by strong acceleration. Note that organic volume (a) and sodium octanoate concentration (b) exhibit symmetrical kinetic behavior.

Starting from this qualitative interpretation, several independent authors have proposed more quantitative approaches. First, Billingham and Coveney [3], then Chimadzhew et al. [4], and later Maestro [5] investigated several macroscopic kinetic models by using exclusively the original BLL experimental results. In these models, the complete autocatalytic process has been artificially divided into two different steps depending on the surfactant concentration being below or above the cmc. None of these models was able to reproduce accurately the effect of added surfactant on the observed kinetics. To address this deficiency, an alternative approach has been proposed by Coveney et al. [6,7]. The principal idea behind this approach is to formulate a global nonequilibrium model wherein all the steps are coupled and without postulating an a priori set cmc. The numerical simulations of this nonequilibrium model show the highly dynamic nature of the entire process, including the reversible self-assembly and breakup of the micelles. Although these models bring new concepts to the literature on reaction kinetics, several basic questions remain unresolved. For example, the possibility of anionic micellar catalysis is questionable because one of the reactants is the negative hydroxide ion OH^-. In these conditions, micellar catalysis is not expected [8]. Another serious limitation of these modeling efforts is the failure to obtain a more accurate quantitative description of the original BLL experiment in order to exclude or validate the proposed mechanism by its ability to fail or fit quantitatively the experimental kinetic curves.

In order to develop a comprehensive and sufficiently realistic kinetic model for the observed autocatalytic behavior, we experimentally revisited [9] the BLL reaction via systematic measurements of the kinetics of

the biphasic hydrolysis of C-4 to C-8 ethyl alkanoates. In all cases, the autocatalytic behavior was observed; that is, there was acceleration of the reaction rate during the course of the reaction. The development of the kinetic model describing such autocatalytic behavior is outlined in Section II. The model has been validated by comparison with experiments in Section III. To reduce the number of free parameters present in the kinetic model, all thermodynamic variables appearing in the model have been theoretically predicted. For this purpose, thermodynamic calculations at 80°C and 3 M ionic strength have been performed to estimate the solubility of ethyl alkanoates in the aqueous medium, the dependence of this solubility on the concentration of reaction products ethanol and sodium octanoate, the cmc of sodium alkanoates, the average size and stoichiometry of aggregates in the presence of ester, and the localization of the ester within the aggregates. The prediction of all these thermodynamic variables is described in Section IV. The last section briefly summarizes the main conclusions. In the following text, the reactions are numbered with the notation re., the physicochemical processes with the notation pr., and the equations with the notation eq.

II. MODELING OF AUTOCATALYTIC BIPHASIC ALKALINE HYDROLYSIS OF ETHYL ALKANOATES

In order to construct a kinetic model, we take into consideration all of the main reactive species and the various macroscopic physicochemical processes that are expected to occur in the oil/water biphasic hydrolysis of long-chain ethyl esters. These liquid-liquid reaction systems can be visualized as consisting of three phases or pseudophases. The organic phase, which is considered to contain only the neat ester, will be denoted as E_{org}.* The aqueous phase initially contains hydroxide and sodium ions, but during the reaction several other species accumulate: dissolved ester (E_{aq}), free surfactant molecules (S^-, denoted as S), ester-containing aggregates (ECAs) that consist of an average of g' surfactants and p ester molecules, empty micelles (M) containing an average of g surfactants, and ethanol (EtOH). In between, we have considered an interfacial pseudophase (E_{int}), which corresponds to a small volume in which the density profiles of ester and water are functions of the distance from their respective bulk phases. E_{int} corresponds to the part of the bulk organic phase that is directly in contact with the aqueous phase. The sequence of events in the biphasic alkaline hydrolysis of C-4 to C-8 ethyl alkanoates in a stirred tank reactor can be summarized by the following six main steps: formation of an ethyl ester–aqueous interface, dissolution of ester in the aqueous phase, hydrolysis of the ester, micellization of product sodium alkanoate, solubilization of ester into micelles, and micelle-mediated transport of ester into the aqueous phase. We will now develop the details of each step.

*Tests using sodium alkanoates or water have shown that their dissolution in the ester phase is negligible. Moreover, 200 Mhz NMR measurements using $CDCl_3$ as solvent have shown that during the reaction the volume ratio of ethanol within this phase always remained less than 8%.

A. Formation of an Ethyl Ester-Aqueous Interface

For an undisturbed oil (ethyl ester)-water interface in a reactor, the number of ester molecules located at the interface (n_{Eint}) can be assumed proportional to the reactor cross section. On applying mechanical stirring, emulsification of oil occurs. This effect increases with increasing agitator speed. Kinetic studies of the emulsification of oil in a continuous water phase have been performed by Polat et al. [10] in a laboratory reactor relatively similar to ours. It was found that dispersion proceeds quite rapidly (with a half-time of the whole process around 1 min) and reaches a steady value asymptotically. In these conditions, n_{Eint} depends on the relative rate of stirring and coalescence, the oil/water volume ratio, and the presence of surfactants. Surfactants are known to decrease the interfacial tension by adsorption at the interface, thereby decreasing the energy needed to break a droplet and creating new interfacial areas. Taking into account all of these parameters that influence the size of the interface, we have suggested an empirical relation for n_{Eint} on phenomenological grounds. See Section III.D.2 [Eq (1)]. We note that a more detailed fundamental study of the interface is beyond the scope of this chapter.

B. Dissolution of Ester in the Aqueous Phase

The saturation solubility $[Solub]_0$ of long-chain alkyl esters in aqueous solution is generally low and decreases appreciably with increasing chain length, similar to the behavior of hydrocarbons in water. Section IV.A provides a brief summary of the thermodynamic relations governing the aqueous solubility of ethyl esters. The solubility of ethyl esters in water is increased by the presence of various additives such as ethanol

and sodium alkanoates that enter the system as the products of the hydrolysis reaction. The increase in the solubility of the ester is due to the so-called solvent or salting-in effects [11]. Thermodynamic treatments of these solubility enhancements due to the solvent and salting-in effects are described in Section IV.B.

Table 1 lists the saturation solubility of the ethyl esters in the aqueous phase $[Solub]_0$, the correcting coefficient α that accounts for the salting-in effect, and the molar volumes of C-4 to C-8 ethyl alkanoates. For simplicity, we have assumed that the solubility enhancement due to ethanol is similar to the salting-in effect and describable by the coefficient α.

From the kinetic modeling point of view, dissolution can be seen as an equilibrium between ester in the bulk organic phase (E_{org}) and ester in the aqueous solution (E_{aq}).

$$E_{org} \rightleftharpoons E_{aq} \qquad \text{(re. 1)}$$

See Sections III.D.3 and III.D.8 (pr. 1) for more details related to this equilibrium.

C. Hydrolysis of Ethyl Ester

We have assumed that the hydrolysis reaction occurs only in the bulk water phase and can be represented as

$$E_{aq} + OH^- \rightarrow S^- + EtOH \qquad \text{(re. 2)}$$

The hydrolysis at the interface region has been neglected because of the expected lack of hydroxide ions in this pseudophase. These simplifying assumptions are supported by the studies of Sharma and Nanda [12] and Engel and Hougen [13], who used ester hydrolysis under biphasic liquid-liquid conditions in order to compare the rate of bulk hydrolysis with the rate of mass transfer across the oil-water interface.

The kinetics of alkaline hydrolysis of ethyl alkanoates have been studied by Evans et al. [14] under monophasic conditions (85% ethanol or 70% acetone in aqueous-organic solvent mixture). It has been found that the second-order rate constants increase with the water content in the reacting medium and that they are almost independent of the carbon chain length. From the reported activation energy and after extrapolation to 100% water solvent, the hydrolysis second-order rate constant in water has been estimated to be around 60 $M^{-1}\ s^{-1}$ at 80°C and 17 $M^{-1}\ s^{-1}$ at 60°C. These rate constants would be significantly modified if the hydrolysis is catalyzed. However, anionic micelles are not known to catalyze basic hydrolysis of long-chain esters because of mutual electrostatic repulsion [15] between the hydroxyl ions and the surfactant anions. Therefore, the rate constants just estimated are applicable to re. (2) in the present model.

D. Micellization of Product Sodium Alkanoates

Following Becker-Döring equations [16] or Aniansson and Wall theory [17], one can represent the micellization process by the stepwise association and dissociation of the micelles (i.e., only one surfactant monomer at a time enters and leaves the micelles):

$$S_{j-1} + S \rightleftharpoons S_j \qquad \text{(re. 3)}$$

where S_j denotes a micellar aggregate containing j surfactant monomers ($j = 2, 3, \ldots$). Assuming monodisperse micelles, the whole set of reversible addition and fragmentation processes can be contracted to a one-step micellization equilibrium. The gth order kinetics reflects the fact that micellization requires (on average) the assembly of g surfactant monomers:

$$gS \rightleftharpoons M \qquad \text{(re. 4)}$$

We have confirmed by numerical simulation that the simplified representation of a multistep aggregation equilibrium by a one-step monomer-micelle equilibrium is satisfactory for our macroscopic modeling of biphasic hydrolysis. This one-step model (re. 4) has the capacity to generate a cmc in a self-consistent manner, i.e., by its own structure.

The equilibrium parameters associated with this one-step model, namely the average micelle aggregation number g and the critical micelle concentration cmc,

TABLE 1 Saturation Solubility $[Solub]_0$, Solubility Enhancement Coefficient α, and Molar Volume of Ester V_m Obtained from Thermodynamic Calculations at 80°C and 3 M Ionic Strength

	C-4	C-5	C-6	C-7	C-8
$[Solub]_0$ (M)	5.49×10^{-3}	1.70×10^{-3}	5.30×10^{-4}	1.60×10^{-4}	5.11×10^{-5}
α (M^{-1})	0.56	0.64	0.71	0.78	0.85
V_m (M^{-1})	0.132	0.149	0.166	0.182	0.199

have been determined on the basis of predictive molecular thermodynamic calculations of aggregate size distributions carried out in nonreactive solutions. These calculations are briefly described in Section IV.C. The predicted size distributions of the sodium alkanoate aggregates are shown in Fig. 2 for chain lengths of C-4 to C-8.

The aggregate size distributions have been calculated for various values of total surfactant concentration. From the size distribution, the weight average aggregation numbers are determined and are plotted as a function of the total surfactant concentration in Fig. 3. This plot can be used to determine the cmc by identifying it as the concentration corresponding to a sharp change in the aggregation number. The cmc values are determined for various surfactant tail lengths to be approximately as follows: C-4, cmc > 3 M; C-5, cmc = 1 M; C-6, cmc = 0.3 M; C-7, cmc = 8.3×10^{-2} M; and C-8, cmc = 2.5×10^{-2} M. The weight average aggregation number (g) has been estimated at a surfactant concentration higher than the cmc for each ethyl ester: C-4, $g < 6$; C-5, $g = 12$; C-6, $g = 24$; C-7, $g = 36$; and C-8, $g = 47$. These results are in accordance with the experiments of Danielsson et al. [18], who demonstrated that association occurs in solutions of alkanoates but only for tails bearing more than four carbon atoms. See Section III.D (pr. 5).

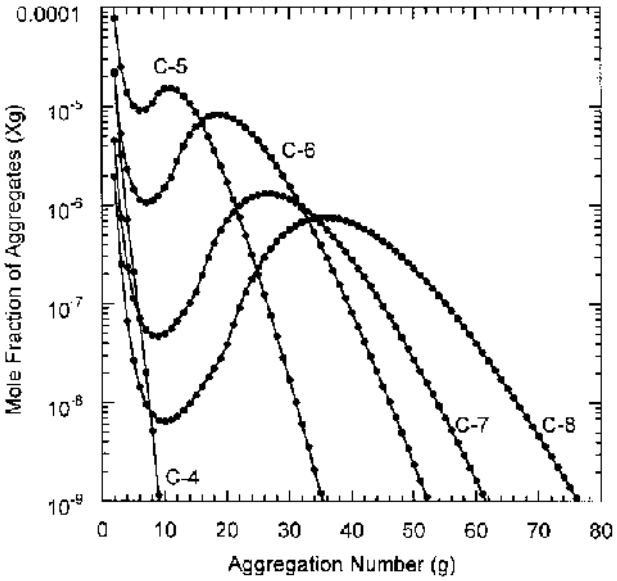

FIG. 2 Mole fraction of aggregates (X_g) versus aggregation number (g) for C-4 to C-8 alkanoates at 80°C and in the presence of 3 M NaCl salt, estimated from thermodynamic calculations. Surfactant concentrations are C-4, 1.15 M; C-5, 0.96 M; C-6, 0.39 M; C-7, 0.112 M; and C-8, 0.058 M. Note that C-4 does not micellize under these conditions.

E. Solubilization of Ester into Micelles

Solubilization refers to the large increase in the amount of solubilizate molecules in aqueous surfactant solutions (far beyond their solubility limit in water) caused by the incorporation of hydrophobic solubilizates into the micelles formed in surfactant solutions. Thermodynamic calculations discussed in Section IV.D show that ester-containing aggregates (ECAs) are formed even at low surfactant concentrations. This is indeed the case at the beginning of reaction, before the critical micelle concentration (corresponding to solubilizate-free conditions) has been reached. These calculations also suggest that the size of ECAs increases as a function of the total surfactant concentration. The increase in aggregate size results from an increase in both the average number of surfactant molecules (g') and the average number of solubilized ester molecules (p) in the micelle. Figure 4 shows the predicted weight average aggregation number of the micelles saturated with the solubilizate (ethyl ester), and Fig. 5 provides the predicted average number of ester molecules solubilized in a micelle.

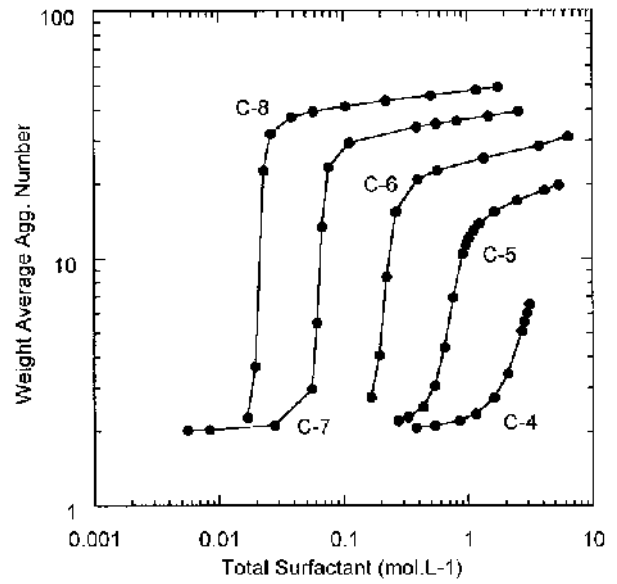

FIG. 3 Weight average aggregation number versus total surfactant concentration of various sodium alkanoates at 80°C and in the presence of 3 M ionic strength, estimated from thermodynamic calculations.

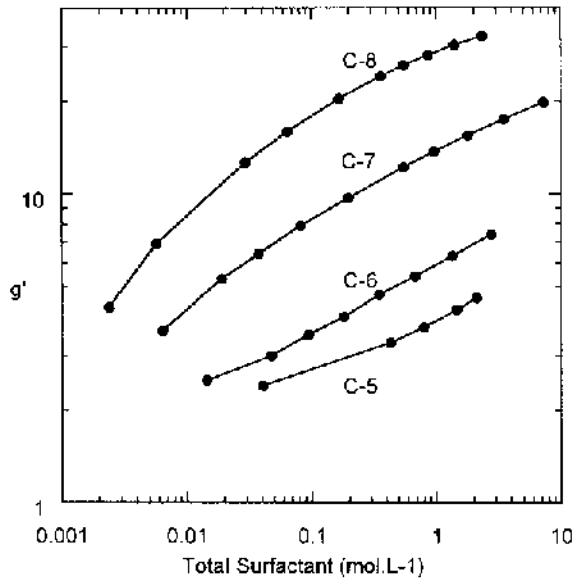

FIG. 4 Weight average aggregation number of micelles (g') in the presence of ester as solubilizate versus total concentration of surfactant at 80°C and in the presence of 3 M ionic strength, estimated from thermodynamic calculations.

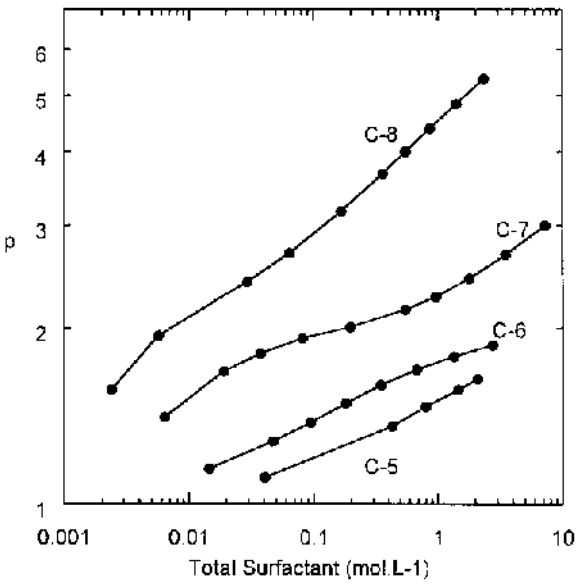

FIG. 5 Average number of ester molecules (p) solubilized in each micelle versus total concentration of surfactant at 80°C and in the presence of 3 M ionic strength, estimated from thermodynamic calculations.

The thermodynamic calculations distinguish between solubilized ester molecules located in the core (where they are protected against hydrolysis) and those in the periphery (where they are more accessible). The predicted molar ratio of the number of solubilized ester molecules in the periphery (namely the surfactant tail region of the aggregate) to that in the core is plotted in Fig. 6 as a function of the average aggregation number of the micelle for various surfactant chain lengths.

For smaller micelles, the ester molecules have a greater tendency to be located in the core. As a result, at the beginning of the reaction, smaller aggregates store ester molecules in the core, where they are protected against hydrolysis. Later, larger aggregates with more ester located in the periphery participate in the phase transfer process. The identification of different regions of micelle where solubilizate molecules can be incorporated has been discussed in the literature. For example, Mukerjee et al. [19] suggested that the interior of a micelle is divided into two regions: the surface region (palisade layer) and the core region. Depending on its polarity, the solubilizate is preferentially solubilized in either of the two regions. Nonpolar molecules such as aliphatic hydrocarbons are solubilized mainly in the core region, and more polar molecules such as

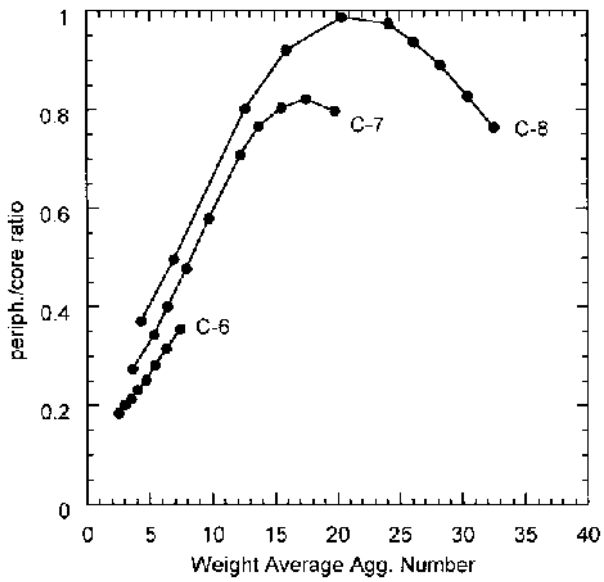

FIG. 6 Distribution of solubilizate ester between the periphery and the core (plotted as the ratio of moles in the periphery to the moles in the core) in sodium alkanoate micelles as a function of the weight average aggregation number. Note that except for C-6 (which generates only small aggregates), the periphery-to-core ratio increases and then decreases for larger micelles.

alcohols are dissolved mainly in the surface layer. The concept of two regions of solubilization has been incorporated in the thermodynamic theory of solubilization formulated by Nagarajan et al. [20] and by Jönsson et al. [21]. It has also been shown [20] that the same solubilizate molecule (for example, an aromatic hydrocarbon) can be located in both the core and the periphery of the micelle depending upon its relative amount in the micelle.

The kinetic mechanism of solubilization of oil into micelles in aqueous medium has been investigated by Karaborni et al. [22] using molecular dynamics simulations. They concluded that (1) there is dissolution of oil in the water phase before oil is captured by micelles, (2) there is exchange of oil between the oil droplet and the micelle during a soft collision, and (3) there is adsorption of surfactants on oil droplets followed by the collective desorption of surfactants and oil from the adsorbed interface. According to Plucinski and Nitsch [23], the solubilization kinetics are controlled by exchange of oil between the oil droplet (E_{org}) and the micelle (ECA) during a soft collision. The rate of solubilization is proportional to the oil solubility in water and increases when the concentration of micelles increases.

For modeling purposes, a one-step solubilization process (i.e., with a high-order kinetic rate) has been used instead of a multistep description, considering, however, two sizes of ECA. Smaller ECAs are characterized as having ester molecules stored in the core, where they are temporarily protected against hydrolysis. Owing to their small size, they show lower cooperativity, i.e., lower kinetic order. On the contrary, larger aggregates exhibit higher cooperativity and more phase transfer possibilities because in this case ester is closer to the periphery. Two parallel solubilization processes with two sizes of ECA and two cooperativities have been taken into account.

$$p_i E_{org} + g_i' S \rightleftharpoons ECA_i \qquad \text{(re. 5)}$$

where p_i and g_i' (i = 1 or 2) are, respectively, the number of ester and surfactant molecules in smaller (i = 1) or larger (i = 2) ECA_i. See Section III.D (pr 3.1 and pr 3.2).

F. Micelle-Mediated Transport of Ester into the Aqueous Phase

Hebrant and Tondre [24] have studied the transport of amino acids through liquid membranes mediated by reverse micelles. They have shown that transport dynamics seem to be governed mostly by the rate of release rather than by the rate of uptake. Kinetics of liquid-liquid extraction by micelles have been investigated by Otsuki and Seno [25]. They concluded that oil molecules transfer across the oil-water interface, diffuse for a while, and then are taken up by micelles and diffuse again. The authors found that the rate of transfer shows a strong correlation with the water solubility of oil. From this literature survey, it appears that ECAs play the role of mass transfer carriers. In these conditions, a process symmetrical with solubilization has been considered in our kinetic modeling approach. ECAs are dispersed in the bulk aqueous phase, where they dissociate releasing g' surfactant and p ester molecules. See section III.D (pr 4.1 and pr 4.2).

$$ECA_i \rightleftharpoons p_i E_{aq} + g_i' S \qquad \text{(re. 6)}$$

III. VALIDATION OF THE MODEL

Several independent experiments have been performed in order to validate the main features of our model described in the previous section.

A. Short-Chain-Length Ester: Ethyl Butanoate (C-4)

Autocatalytic kinetic behavior has been observed experimentally in the hydrolysis of ethyl butanoate, the concentration range used for this experiment being 0 to 1.8 M. Because sodium butanoate is known not to form aggregates in this concentration range, the three steps of micellization, solubilization, and micelle-mediated transport of ethyl ester are not relevant to understanding the observed kinetics. Under these conditions, the observed autocatalysis can be attributed only to salting-in and solvent effects.

At the beginning of the reaction, the rate-determining step is the dissolution process. The rate does not depend on the available quantity of oil. Hydrolysis thus takes place as soon as some ester is present in the aqueous phase. As the reaction proceeds, the products sodium butanoate and ethanol accumulate in the water phase. Consequently, the concentration of the ethyl ester in the aqueous phase increases because of the salting-in effect due to sodium butanoate and the solvent effect due to ethanol. The rate of dissolution of the ester increases continuously until all the organic phase has disappeared. One can observe from Fig. 7 that model simulations performed taking only the first three kinetic steps postulated in Section III describe quantitatively the experimental kinetic results.

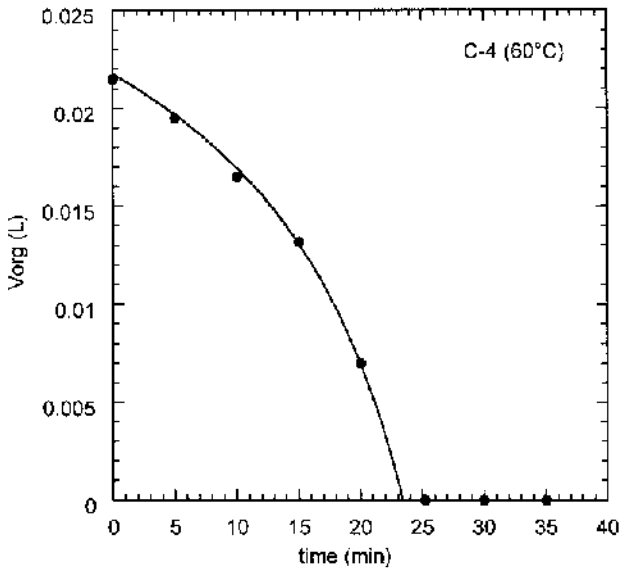

FIG. 7 Evolution of the volume of the organic phase in the biphasic hydrolysis of ethyl butanoate using 3 M NaOH aqueous solution. $T = 60°C$, $V_{org0}/V_{tot} = 22\%$, stirring rate 800 rpm in a round-bottom flask. (●) Experimental points; (——) simulation by the model; only one parameter has been fitted: $k_{-1} = 5.15 \times 10^{-1}\ s^{-1}$.

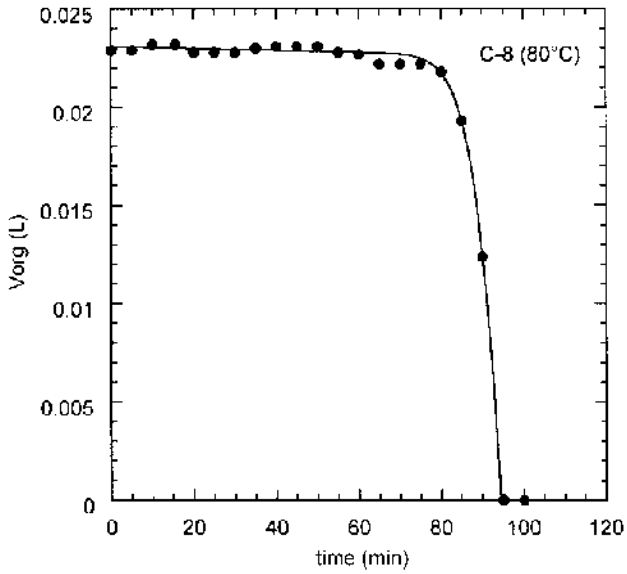

FIG. 8 Evolution of the volume of the organic phase in the biphasic hydrolysis of ethyl octanoate in a 250-mL round-bottom flask using 3 M NaOH aqueous solution. $T = 80°C$, $V_{org0}/V_{tot} = 22\%$, stirring rate 800 rpm. (●) Experimental points; (——) simulation by the model. Fitted parameters are $k_{32} = 2.87 \times 10^{41}$; $k_{-32} = 2.3 \times 10^{-2}$; $k_{42} = 1.56$; $k_{-42} = 10^{-10}$; $k_{-5} = 10^{-13}$; k_{-1} has the same value as in C-4.

B. Long-Chain-Length Ester: Ethyl Octanoate (C-8)

The reaction with ethyl octanoate shows a much more pronounced nonlinear behavior than that observed in the case of ethyl butanoate. In particular, the acceleration of the reaction rate that follows a long induction time is much stronger and abrupt. Solvent and salting-in effects are far from being sufficient to explain this strong acceleration behavior. Indeed, the contributions to autocatalysis from solvent and salting-in effects are considerably smaller (compared with the case of ethyl butanoate) because of the much lower solubility of ethyl octanoate in water, as noted previously (see Table 1). The role of ECAs must be taken into account to explain the observed autocatalysis. The ECAs ensure solubilization of ethyl octanoate in the micelles and thereby facilitate the phase transfer of ethyl octanoate from the organic to the aqueous phase, where it is rapidly hydrolyzed, releasing more and more surfactant molecules in the water phase. Figure 8 shows the result of simulations based on the model in which all the kinetic steps postulated in Section II have been included.

The model shows good quantitative agreement with the experimental data. Considering two sizes for ECAs is not necessary for a satisfactory fitting. After an induction period, during which surfactant molecules accumulate to reach a critical aggregation concentration, phase transfer mediated by ester-containing aggregates takes place and strong acceleration is observed. Finally, when all the ester has been consumed, empty micelles are formed.

C. Medium-Chain-Length Ester: Ethyl Hexanoate (C-6)

In this case, the kinetic data shown in Fig. 9 are characterized by a significant initial slope and by a large reaction extent (about 30% of ester is consumed) before any marked acceleration starts; autocatalysis seems to be inhibited for a while.

Our first attempts to fit the experimental kinetic curves using salting-in and solvent effects and only one size for the ECAs (as was done for C-8 ester hydrolysis) met with various difficulties. Specifically, if we try to reproduce the initial slope, then the overall reaction time is found to be too short, phase transfer then taking place too early in the reaction. On the other hand, if we attempt to obtain the correct overall reaction, then the initial rate becomes too small (shown as dashed line in Fig. 9). Considering only one size for

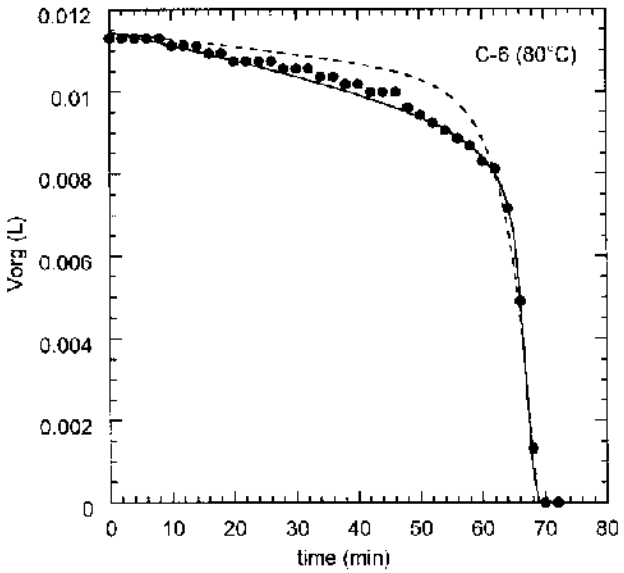

FIG. 9 Kinetics of ethyl hexanoate biphasic hydrolysis performed in a 18.9 cm^2 section cylindrical flask at 600 rpm and T = 80°C, V_{org} = 11.5 mL; V_{tot} = 50 mL. (●) Experimental points; (dashed line) best fit assuming only one size of aggregates; (continuous line) best fit assuming two sizes of aggregates. Fitted parameters are $k_1 = 116$; $k_{3.1} = 2.07 \times 10^6$; $k_{-3.1} = 64.3$; $k_{4.1} = 0.06$; $k_{-4.1} = 9.82$; $k_{3.2} = 8.19 \times 10^7$; $k_{-3.2} = 9.83 \times 10^3$; $k_{4.2} = 137$; $k_5 = 1.52 \times 10^{-4}$; Stir = 183; β = 128.

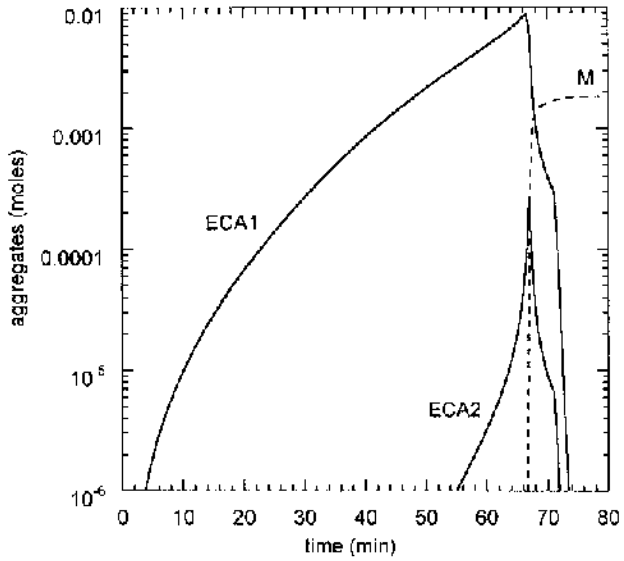

FIG. 10 Numerical simulation of the evolution of aggregates ECA_1, ECA_2, and M during biphasic hydrolysis of ethyl hexanoate. Fitted parameters are the same as in Fig. 9. Note that although the acceleration period occurs around 30% extent (a value close to the cmc of sodium hexanoate in our experimental conditions), empty micelles (M) appear only at the end of reaction.

the ECAs is therefore clearly not sufficient to describe the observed C-6 kinetics accurately. It is necessary to assume two sizes for the aggregates: ECA_1 (the smaller) are formed early in the reaction with low cooperativity and accumulate ester molecules protected from hydrolysis; ECA_2 (the larger) are formed later with higher cooperativity and contribute significantly to phase transfer. Figure 10 shows that smaller aggregates play the role of a storage reservoir.

To get further insight into this phenomenon, several complementary experiments were carried out. Experiments without emulsifying the mixture (i.e., with a well-defined interface) show that the extent of reaction before acceleration is not affected by the size of the interface (Fig. 11).

These experiments show that the size of the interface does have an effect on the overall reaction time, but they allow us to exclude any ''storage'' effect due to large adsorption at the interface. To check the initial volume and stirring effects, several other experiments were carried out with decreasing initial volume of ester, from 11.4 mL (0.069 mol) to 2.6 mL (0.016 mol). Because 30% extent of reaction (observed before any ac-

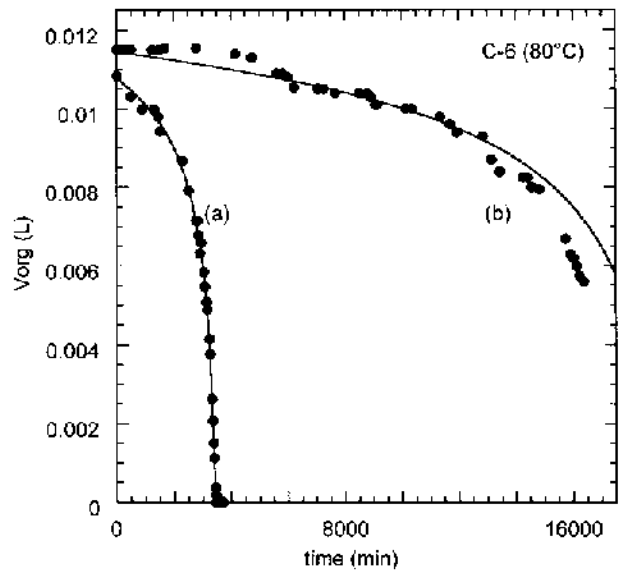

FIG. 11 Kinetics of ethyl hexanoate biphasic hydrolysis in nonemulsified conditions (Stir = 0). (a) Int_0 = cross section, Int_0 = 18.9 cm^2; (b): Int_0 = 3.3 cm^2. Fitted parameters are the same as in Fig. 9 except $k_{3.2} = 8.19 \times 10^7$; $k_{4.2} = 137$.

celeration effects) corresponds to 0.021 mole of ester consumed, one would expect no significant acceleration to be observed for experiments in which the initial number of moles of ester is smaller than this value. As shown in Fig. 12 (kinetic curves a, d, e, and f), this is indeed what is observed experimentally: the experiments (a, d, and e) show a marked acceleration around 30% extent, but the experiment (f) involving less than 0.021 mole of ester does not. Moreover, the overall reaction time increases as the initial volume of the organic phase decreases. It is suggested that this phenomenon is related to the dependence of reaction time on the size of the interface. Assuming that when the stirring rate is maintained constant (600 rpm), the size of the droplets formed by emulsification remains the same, decreasing the organic phase volume decreases the number of ester droplets and hence the interface size and therefore the overall reaction time increase. Finally, we carried out two more experiments using faster stirring rates. The kinetic curves obtained support the preceding interpretation. As expected, as the stirring rate is increased, the reaction time decreases (Fig. 12a, b, and c).

Kinetic analysis of the biphasic hydrolysis of C-5 and C-7 ethyl alkanoates has not yet been performed using the model with two aggregate sizes. But preliminary studies show that the interpretation of the kinetics of the C-5 experiments requires consideration of both salting-in and solvent effects or low cooperative phase transfer by only one size of ECA. In this particular case it can be shown that salting-in and low cooperative phase transfer have similar consequences for the observed kinetics. For C-7 experiments, it has been shown that as in the C-8 case, high-order cooperative formation of one size of ECA is the predominant process. Improvement of the fit is, however, obtained by considering a few percent of stored ester (for instance, in the smaller ECA_1 aggregates).

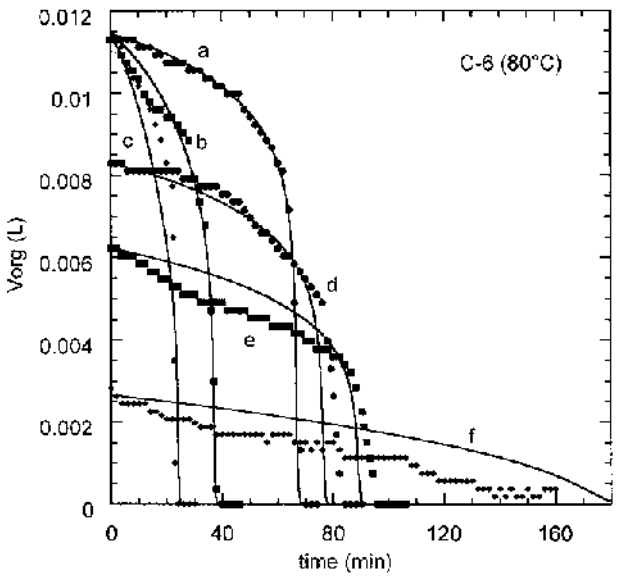

FIG. 12 Effect of initial organic volume (a) = 11.4 mL, (d) = 8.3 mL, (e) = 6.2 mL, (f) = 2.6 mL and stirring rate (a), (d), (e), and (f) = 600 rpm, (b) = 800 rpm, (c) = 1050 rpm on the kinetics of the biphasic hydrolysis of ethyl hexanoate at 80°C. Fitted parameters are the same as in Fig. 9 except for (a), (d), (e), and (f) Stir = 183; (b): Stir = 497; (c): Stir = 1013.

D. Skeleton Mechanism, Rate Laws, and Kinetic Parameters

More details of the kinetic model just discussed are given in this section. The details include notations, reaction schemes, reaction rate expressions, and assumptions made to simplify the kinetic model.

1. List of Species

E_{org}: ethyl alkanoate in the bulk organic phase
E_{aq}: ethyl alkanoate dissolved in the bulk aqueous phase
OH^-: hydroxide ion
S: free sodium alkanoates in the bulk aqueous phase
EtOH: ethanol
ECA_1: smaller ester-containing aggregates made up of g_1' surfactants and incorporating p_1 ester molecules in the core
ECA_2: larger ester-containing aggregates made up of g_2' surfactants and incorporating p_2 ester molecules in the periphery
M: empty micelles made up of g surfactants

2. List of Variables

$$n_{Eint} = (Int_0/s_0)(1 + Stir(V_{org}V_{aq}/V_{tot}^2))(1 + \beta(n_S/V_{aq})) \quad \text{(eq. 1)}$$

n_X = number of moles of species x
n_{Eint} = number of ethyl ester molecules at the aqueous-organic interface.

3. Processes and Rate Laws

$E_{org} \rightleftharpoons E_{aq}$	$r_1 = k_1 n_{Eint} \exp(\alpha(n_{EtOH} + n_S)/V_{aq})$	(pr. 1)
	$r_{-1} = k_{-1} n_{Eint} n_{Eaq}/V_{aq}$	
$E_{aq} + OH^- \rightarrow S + EtOH$	$r_2 = k_2 n_{Eaq}(n_{OH^-})/V_{aq}$	(pr. 2)
$p_1 E_{org} + g_1' S \rightleftharpoons EAC_1$	$r_{3.1} = k_{3.1} n_{Eint}(n_S/V_{aq})^{g_1'}$	(pr. 3.1)
	$r_{-3.1} = k_{-3.1} n_{ECA_1}$	

$$\mathrm{ECA}_1 \rightleftharpoons p_1\mathrm{E}_{aq} + g_1'\mathrm{S} \quad r_{4.1} = k_{4.1} n_{\mathrm{ECA}_1} \qquad \text{(pr. 4.1)}$$

$$r_{-4.1} = k_{-4.1} n_{\mathrm{Eaq}} (n_S/V_{aq})^{g_1'}$$

$$p_2\mathrm{E}_{org} + g_2'\mathrm{S} \rightleftharpoons \mathrm{ECA}_2 \quad r_{3.2} = k_{3.2} n_{\mathrm{Eint}} (n_S/V_{aq})^{g_2'} \qquad \text{(pr. 3.2)}$$

$$r_{-3.2} = k_{-3.2} n_{\mathrm{ECA}_2}$$

$$\mathrm{ECA}_2 \rightleftharpoons p_2\mathrm{E}_{aq} + g_2'\mathrm{S} \quad r_{4.2} = k_{4.2} n_{\mathrm{ECA}_2} \qquad \text{(pr. 4.2)}$$

$$r_{-4.2} = k_{-4.2} n_{\mathrm{Eaq}} (n_S/V_{aq})^{g_2'}$$

$$g\mathrm{S} \rightleftharpoons \mathrm{M} \quad r_5 = k_5 n_S^g V_{aq}^{1-g} \qquad \text{(pr. 5)}$$

$$r_{-5} = k_{-5} n_M$$

where r_j is the rate of process j (in mol min^{-1}), rate constant k_j is expressed in the usual units (i.e., in L^{g-1} mol^{1-g} min^{-1} for a gth order reaction), index -j refers to the reverse process j.

4. Kinetic Parameters

Rate constants: first order: k_1, $k_{-3.1}$, $k_{4.1}$, $k_{-3.2}$, $k_{4.2}$, k_{-5}
Second order: k_{-1}, k_2
Higher order: $k_{3.1}$ and $k_{-4.1}$ ($g_1 + 1$), $k_{3.2}$ and $k_{-4.2}$ ($g_2 + 1$), k_5 (g)
Relationships between kinetic parameters:

$$k_1 = k_{-1}[\mathrm{Solub}]_0$$

$$k_5 = k_{-5}\ \mathrm{cmc}^{1-g}/g^2 \qquad \text{(Benjamin's formula [26])}$$

5. Thermodynamic Parameters

S_0: molecular area of ethyl alkanoates (around 10^4–10^5 m^2 mol^{-1})
V_m: molecular volume of ethyl alkanoates
$[\mathrm{Solub}]_0$: saturation solubility of ethyl alkanoates in aqueous phase
cmc: critical micelle concentration of sodium alkanoates
α: correction factor for salting-in or solvent effects
β: interfacial tension correction factor
g: average aggregation number of empty micelles
g_i': average number of surfactant molecules in ester-containing aggregates ECA_i
p_i: average number of ester molecules in an ester-containing aggregate ECA_i

6. Experimental Parameters

Int_0: cross section of the undisturbed interface (no emulsification in experiments)
Stir: rate of stirring (emulsification in experiments)
$V_{org} = V_m n_{Eorg}$ (volume of the organic phase)
$V_{aq} = V_{tot} - V_{org}$ (volume of the aqueous phase)
V_{tot} = total volume (oil + water)

7. Differential Equations

The whole set of differential equations has been built according to the matrix of the stoichiometric coefficients listed in Table 2.

8. Comments on Eq. (1) and Rate Laws

(*a*) *n_{Eint} and Interface Area.* n_{Eint} is given by the empirical Eq. (1). The nondimensional term $V_{org}V_{aq}/(V_{tot})^2$ accounts for the dependence of the interface area on the volume fractions of both organic (V_{org}/V_{tot}) and aqueous phases (V_{aq}/V_{tot}). We have assumed a quasi-steady-state value for the size of the interface and we have also used a linear dependence on the Stir parameter representing the intensity of mixing and the β parameter representing the influence of interfacial tension on the interfacial area generated.

(*b*) *Dissolution Rate of Ethyl Ester in Aqueous Phase: r_1 and r_{-1}.* The overall rate (i.e., the time constant to reach the saturation solubility) has been taken to be proportional to n_{Eint}. As the saturation solubility does not depend on the size of the interface, this factor has been put in both dissolution and release rate. The dissolution rate also depends on the concentration of the reaction products, both surfactant (salting-in effect) and ethanol (solvent effect), and follows an exponential law. Because solubility is independent of the available

TABLE 2 Matrix of the Stoichiometric Coefficients of the Whole Mechanism

d/dt	r_1	r_{-1}	r_2	r_{31}	r_{-31}	r_{32}	r_{-32}	r_{41}	r_{-41}	r_{42}	r_{-42}	r_5	r_{-5}
n_{Eorg}	−1	1	0	$-p_1$	p_1	$-p_2$	p_2	0	0	0	0	0	0
n_{Eaq}	1	−1	−1	0	0	0	0	p_1	$-p_1$	p_2	$-p_2$	0	0
n_{OH^-}	0	0	−1	0	0	0	0	0	0	0	0	0	0
n_S	0	0	1	$-g_1'$	g_1'	$-g_2'$	g_2'	g_1'	$-g_1'$	g_2'	$-g_2'$	$-g$	g
n_{EtOH}	0	0	1	0	0	0	0	0	0	0	0	0	0
n_{ECA1}	0	0	0	1	−1	0	0	−1	1	0	0	0	0
n_{ECA2}	0	0	0	0	0	1	−1	0	0	−1	1	0	0
n_M	0	0	0	0	0	0	0	0	0	0	0	1	−1

First column corresponds to the rate of evolution dn_X/dt of the species X in mol min^{-1} units. See text for values of p_i, g_i', and g. For example, the differential equation for the first species in the table will be $dn_{Eorg}/dt = -r_1 + r_{-1} - p_1 r_{31} + p_1 r_{-31} - p_2 r_{32} + p_2 r_{-32}$.

quantity of solute, the rate law r_1 is zeroth order with respect to n_{Eorg}.

(*c*) *Rate of Aggregation: $r_{3.1}$ and $r_{3.2}$.* In order to account for the different properties of small and large aggregates during the C-6 reaction course where surfactant concentration varies from 0 to 1.38 M, we have taken two extreme values of p and g' from Figs. 4 and 5. Noting that at low surfactant concentrations only molecular clusters such as dimers and trimers are likely, we have chosen $p_1 = 1$ and $g_1' = 2$ for ECA_1 (this corresponds to a surfactant concentration of 0.01 M at the beginning of the reaction) and $p_2 = 2$ and $g_2 = 6$ for ECA_2 (corresponding roughly to a surfactant concentration of 1.0 M at the end of reaction). Aggregation processes are assumed to be gth order (g, g_1', or g_2') in surfactant concentration. Rate laws $r_{3.1}$ and $r_{3.2}$ are zeroth order in n_{Eorg} and first order in n_{Eint} because the more the organic phase is in contact with the water bulk, the faster the exchange occurs.

(*d*) *Micelle-Mediated Transport of Ethyl Ester: $r_{4.1}$ and $r_{4.2}$.* The dissociation rate of ECA has been taken to be first order. Rate laws $r_{-4.1}$ and $r_{-4.2}$ have been taken first order in n_{Eaq}. Stoichiometric coefficients p have been used in the mass balance equations.

IV. THEORETICAL ESTIMATION OF THERMODYNAMIC PARAMETERS

In formulating the model for autocatalysis, a number of thermodynamic variables appear, including the solubility $[\text{Solub}]_0$ of ethyl alkanoates in aqueous solution, the constant α accounting for the influence of ethyl alcohol and sodium alkanoate on the aqueous solubility of ethyl alkanoate, the average aggregation number g of a solubilizate-free micelle M, the critical micelle concentration (cmc), and the number g' of surfactant molecules and p' of ethyl alkanoate molecules in the ECA. These thermodynamic variables (listed in Table 2 or shown in Figs. 3 to 6) have not been treated in our work as free fitting parameters of the kinetic model but instead have been calculated a priori from molecular properties using molecular thermodynamic approaches. Methods of estimation of these thermodynamic variables are briefly described next.

A. Solubility of Ethyl Alkanoates in Water

The experimental solubility data of ethyl alkanoates in water at 298 K have been correlated [27] as a function of the number N of carbon atoms in the alkanoate ($N = 8$ for octanoate). One obtains $\Delta G_S^\circ = 1.317 + 0.688$ N, expressed in units of kcal/mol K, where ΔG_S° is the free energy change associated with dissolution and is equal to $RT \ln X$, where X is the mole fraction solubility of the ester in water. Experimental data on the dependence of solubility on temperature and salt concentration for ethyl alkanoates are not available. Therefore, the corrections for temperature and salt effects have been made using information available for alkanes. The corrections are made using a group contribution procedure and account for all the CH_2 and CH_3 groups in the ethyl alkanoate but ignore any correction for the COO group. In the presence of NaCl, the free energy $\Delta G_S^\circ/RT$ is estimated [28] to change by $0.384C$ for the CH_3 group and by $0.064C$ for the CH_2 group, where C is the molar concentration of the added salt. We do not have information about this correction term at other temperatures, and therefore this correction is taken as temperature independent. From solubility data for alkanes [27] we know that $\Delta G_S^\circ/RT$ for the CH_2 group is 1.496 at 298 K and 1.311 at 353 K. For the CH_3 group, $\Delta G_S^\circ/RT$ is 3.536 at 298 K and 3.548 at 353 K. Therefore the change in temperature from 298 to 353 K will cause a change in solubility given by $\Delta G_S^\circ/RT$ of -0.185 for CH_2 and 0.012 for CH_3. Taking into account the salt and temperature effects on solubility, we can calculate the solubility at 353 K and 3 M NaOH using the solubility information at 298 K and 0 M NaOH as follows:

$$\begin{aligned}\ln X(T = 353\text{ K}, C = 3\text{ M}) = \ln X(T = 298\text{ K}, C = 0\text{ M}) \\ + [0.185n_{CH_2} - 0.012n_{CH_3}] \\ - C[0.064n_{CH_2} + 0.384n_{CH_3}]\end{aligned}$$

The first correction term is for the temperature dependence and the second is for the salt dependence. The numbers of methylene and methyl groups in ethyl alkanoate are denoted by n_{CH_2} and n_{CH_3}, respectively. The mole fraction solubility data X are converted to molar concentration $[\text{Solub}]_0$ by multiplying by 55.55.

B. Solubility Enhancement due to Ethyl Alcohol and Sodium Alkanoate

The solubility of ethyl alkanoate in water is affected by the presence of ethyl alcohol and sodium alkanoate, both of which are products of the hydrolysis reaction. Both contribute to an increase in the aqueous solubility of ethyl alkanoates by modifying the structure of water. To describe the influence of ethyl alcohol, we can view the problem as that of the solubility of ethyl alkanoate in a mixed solvent consisting of ethyl alcohol and water. The solubility in the mixed solvent (X_{mix}) can be represented in terms of the solubility in the pure sol-

vents water and ethanol (X_W and X_E) by applying the framework of any suitable solution theory. For example, application of the Flory-Huggins solution model yields (eq. 3) [29]

$$\ln X_{mix} = \phi_W \ln X_W + \phi_E \ln X_E + \chi_{WE}\phi_E\phi_W \qquad \text{(eq. 3)}$$

where ϕ_W and ϕ_E denote the volume fractions of water and ethanol in the mixed solvent, and χ_{WE} is the interaction parameter between water and ethyl alcohol. Because the volume fraction of ethyl alcohol that would be present under the reaction conditions is small (for example, 1 M ethyl alcohol would represent a volume fraction of about 0.06) and the interaction parameter term is smaller than the other terms, the solubility X_{mix} can be approximately represented by the expression (eq. 4)

$$X_{mix} \approx X_W \exp\left(\phi_E \ln \frac{X_E}{X_W}\right) =$$

$$X_W \exp\left(0.0585 C_E \ln \frac{X_E}{X_W}\right) = X_W \exp(\alpha C_E) \qquad \text{(eq. 4)}$$

In obtaining the preceding expression, we have replaced ϕ_E by $0.0585C_E$, where C_E is the molar concentration of ethanol and α denotes the coefficient of C_E appearing within the exponent. The solubilities X_E and X_W are calculated using known group contributions at 25°C, namely $-0.178\ kT$ and $-0.935\ kT$ for CH_2 and CH_3 groups when ethanol is the solvent and $-1.425\ kT$ and $-3.875\ kT$ when water is the solvent. The group contribution for the COO group can be estimated for water using available solubility data, but such information is unknown in the case of ethanol as the solvent. One may anticipate that the contributions for both water and ethanol would be comparable given their affinity for the polar COO group. Consequently, the ratio X_W/X_E would not be affected significantly by the COO group contribution. Also, the temperature dependences of X_E and X_W would approximately cancel each other and thus to a first approximation, α is temperature independent.

The influence of sodium alkanoates on the solubility of ethyl alkanoates can be described by the concepts of salting in and salting out applied to solutions containing electrolytes. One can write the solubility in the presence of an electrolyte as a function of the electrolyte concentration using the relation of the form (eq. 5)

$$\ln\left(\frac{X(C)}{X(C=0)}\right) = kC \qquad \text{(eq. 5)}$$

where k is the salting-in or salting-out equilibrium constant and C is the molar concentration of the added salt. For inorganic ions, k in the preceding expression is a negative constant and the solute is salted out, implying that its solubility is lowered by the addition of salt. For an organic electrolyte (sodium alkanoate in the present case), depending on the importance of the organic part, the constant k can be positive and the solute is thus salted in, implying that its solubility is enhanced by the addition of the organic salt.

Quantitative methods for determining the salting-in constant k are not sufficiently well developed. Experimental estimates for k based on measured solubility data are thus more commonly used. In principle, k will depend on the organic ion as well as the solute molecule. The equilibrium constant k has been found to increase linearly with the alkyl chain length for large organic ions. For benzoic acid as the solute with long-chain quaternary ammonium ions, it has been found that k has a methylene group contribution of 0.07 M^{-1}. The absolute values of k lie in the range of 0.35 to 0.91 M^{-1} for total carbon numbers of 4 to 12 in the ammonium ions. We observe that the incremental variation in the parameter α that accounts for the influence of ethanol on the solubility of ethyl alkanoates is also 0.07 per methylene group (see Table 2). Because no direct measurements of k relevant to our system are presently available and the incremental variation in α compares with that in k, we assume that α can be equated to k for simplifying our calculations. Therefore, the solubility X of ethyl alkanoates in the presence of ethanol and sodium alkanoate can be written as (eq. 6)

$$X = X(\text{EtOH} = 0,\ \text{S} = 0)\exp\ \alpha([\text{EtOH}] + [\text{S}]) \qquad \text{(eq. 6)}$$

where [EtOH] and [S] are the molar concentrations of ethanol and sodium alkanoate in the aqueous solution.

C. Micellization Variables *g*, cmc, and K_m for Sodium Alkanoates

The aggregation characteristics of sodium alkanoates ($C_{n-1}H_{2n-1}COONa$) such as the cmc, the average aggregation number of micelles, the variance of the micelle size distribution, and the micellization equilibrium constant (step 8 in the reaction scheme) can all be predicted a priori using the molecular thermodynamic theory formulated by Nagarajan and Ruckenstein [30]. For a surfactant solution containing micelles of various aggregation numbers g, the equilibrium condition of a minimum in the Gibbs free energy stipulates (eq. 7)

$$\mu_g^\circ + kT \ln X_g = g(\mu_1^\circ + kT \ln X_1) \qquad \text{(eq. 7)}$$

where X_1 and X_g are the mole fractions of the singly dispersed molecules and aggregates of size g, respec-

tively and μ_1° and μ_g° are their respective standard chemical potentials, defined as those corresponding to infinitely dilute solution conditions. In order to calculate X_g, we need an explicit expression for

$$\Delta\mu_g^\circ = \frac{\mu_g^\circ}{g} - \mu_1^\circ \qquad \text{(eq. 8)}$$

which is the difference in the standard chemical potential between a surfactant molecule in an aggregate of size g and a singly dispersed surfactant molecule in the solvent as a function of the size and shape of the micelles.

From a geometrical point of view, micelles of small aggregation numbers pack as spheres and larger micelles pack into globular or ellipsoidal shapes. The geometrical properties of the spherical and ellipsoidal micelles are dependent only on the aggregation number g and have been described before [30]. The standard state free energy difference term $\Delta\mu_g^\circ$ has a number of contributions that arise from the changes accompanying the aggregation process. These contributions account for the following factors: (1) the surfactant tail is removed from contact with the solvent and is transferred to the hydrophobic core of the micelle $(\Delta\mu_g^\circ)_{tr}$, (2) the surfactant tail inside the micelle has a conformation different from that in a pure hydrocarbon liquid because of packing constraints imposed inside the micelle $(\Delta\mu_g^\circ)_{def}$, (3) the formation of the micelle creates an interface between the hydrophobic micellar core and the solvent $(\Delta\mu_g^\circ)_{int}$, (4) the polar headgroups of the surfactants at the micelle surface exhibit steric repulsions $(\Delta\mu_g^\circ)_{ste}$, and (5) the polar headgroups also exhibit at the micelle surface mutual electrostatic repulsions $(\Delta\mu_g^\circ)_{ionic}$. These expressions are functions of temperature T, the molar concentration of added electrolyte C_{add}, and the micellar size (represented by the aggregation number g).

The molecular constants necessary for the predictive calculations are estimated from the molecular structure of sodium alkanoates. The molecular volume v_s and the extended length l_s of the surfactant tail is calculated [30] from the group contributions of methylene groups and the terminal methyl group. Only two molecular constants specific to a headgroup are needed. One is the cross-sectional area a_p of the headgroup, which is estimated to be 0.11 nm^2 for sodium alkanoates. The other is the distance from the hydrophobic core surface to the position where the counterion is located, which is estimated as $\delta = 0.555$ nm.

All the predicted results correspond to the experimental conditions of 80°C and the presence of 3 M NaCl in the surfactant solution. The predicted weight-average aggregation number g as a function of the total concentration X_{tot} $(=X_1 + \Sigma\, gX_g)$ of sodium alkanoate in solution is plotted in Fig. 3. The mole fractions X are converted to molar concentrations C by multiplying by 55.5. One may notice that for C-4 alkanoate, no aggregate formation occurs up to a surfactant concentration of 2 M. For other tail lengths, one can observe that the aggregation number is increasing with increasing surfactant concentration. This is a typical behavior anticipated [30] when the aggregation numbers are small. Indeed, this behavior corresponds to the presence of a somewhat polydispersed distribution of aggregates in solution. The aggregation numbers listed in Table 2 are the values predicted corresponding to a concentration of 1 M sodium alkanoate. A sharp transition in the plot of X_1 against the total concentration $X_{tot} = X_1 + \Sigma\, gX_g$ is used to predict the cmc values listed in Table 2.

D. Solubilization Variables g' and p

When sodium alkanoates and ethyl alkanoates are both present, solubilizate (ethyl alkanoate) containing aggregates (designated as ECA in the kinetic model) can form at surfactant concentrations that are lower than the cmc calculated for solubilizate-free surfactant solutions. To predict the aggregation number g' and the number of solubilizate molecules p present in an ECA aggregate, one can adopt [30] exactly the same approach as that used for micelle formation. The concentration of aggregates made up of g surfactant molecules and j solubilizate molecules can be written by analogy with the micelle size distribution equation

$$X_g = X_1^g f^{j/g} \exp - \left(\frac{g\Delta\mu_g^\circ}{kT}\right), \qquad \text{(eq. 9)}$$

$$\Delta\mu_g^\circ = \frac{\mu_{gj}^\circ}{g} - \mu_1^\circ - \frac{j}{g}\,\mu_\circ^H, \qquad f = \frac{X_1^\circ}{X_{1\circ}^S}$$

where μ_{gj}° is the standard chemical potential of an aggregate containing g surfactant and j solubilizate molecules, X_g is a function of both g and j, the chemical potential of the solubilizate in the pure solubilizate phase is $\mu_\circ^H$, $X_{1\circ}^S$ is the saturation solubility of the solubilizate in water, and f is the fractional saturation of the solubilizate in water. The molar solubilization ratio corresponding to the maximum solubilization possible is obtained by taking $f = 1$ in the preceding equation. This condition occurs when there is an excess phase of solubilizate coexisting with the aqueous solution. This is the case for our experiment, and the predicted results

thus correspond to the condition $f = 1$. Knowing the distribution X_g as a function of g and j, the average aggregation number g' and the average number of solubilizate molecules p in an aggregate can be calculated.

The factor $\Delta\mu_g^\circ$ is the difference in the standard chemical potential for a surfactant molecule and (j/g) solubilizate molecules present in an aggregate with respect to a singly dispersed surfactant molecule in water and (j/g) solubilizate molecules in the bulk solubilizate phase. All the free energy contributions considered for micelle formation are relevant for the micelles containing the solubilizate, with the understanding that the geometrical properties of the aggregates are now influenced by the number of solubilizate molecules present. Further, the presence of the solubilizate modifies the interfacial tension between the micelle core and water. Also, one has to consider the entropy and the enthalpy of mixing of solubilizate and surfactant molecules in the micelle. Detailed quantitative expressions for such free energy contributions have been formulated before [30] along with geometrical relations for aggregates containing the solubilizates.

The calculated results for g' and p are plotted in Figs. 4 and 5 as functions of the total concentration of sodium alkanoate in solution. One can notice that both g' and p are dependent on the total concentration of the surfactant and increase with increasing surfactant concentration. As mentioned before, this is a feature characteristic of systems in which the aggregation numbers are small. The values listed in Table 2 that are used in the kinetic model are those predicted at a total surfactant concentration of 1 M. The solubilization model considers that some solubilizate molecules are present in the inner core of aggregates, constituting a pure pool of solubilizates, and the remaining solubilizate molecules are distributed in the region of the surfactant tail where they mix and interact with the tails (periphery). The calculated distribution of solubilizate molecules between the periphery and core regions of the aggregates is plotted in Fig. 6.

V. CONCLUSIONS

The mechanism of the biphasic hydrolysis of ethyl alkanoates has been established using thermodynamic calculations and kinetic modeling. The origin of the autocatalytic effect depends on the chain length of the ethyl ester. In the case of ethyl butanoate, the autocatalysis results from the enhancement of ester solubility caused by the reaction products sodium butanoate and ethanol, which are responsible for salting-in and solvent effects. For ethyl octanoate, phase transfer mediated by ester-containing aggregates is the main reason for the occurrence of autocatalytic behavior. In the case of esters of intermediate chain length (ethyl hexanoate), phase transfer is also the main autocatalytic process, but two sizes of ester-containing aggregates need to be invoked to explain phase transfer inhibition in the beginning of the reaction. Small aggregates temporarily store ester, and larger ones transport it into the aqueous phase, where rapid hydrolysis takes place. Pure micelles are formed as the final product when ester has been totally consumed; they have to be considered as an inactive end product. Although we are aware that drastic simplifications have been made, we think that the main reacting species, paths, couplings, and features of the mechanism have been correctly identified.

As a general property, the rate of oil-water biphasic reaction is independent of the remaining amount of supernatant organic phase. As a consequence, biphasic liquid-liquid reactions display intrinsically zero-order kinetics. If the reaction products are able to change the physicochemical properties of the medium, for instance, by increasing the saturation solubility of the organic solute into the aqueous phase, autocatalytic behavior is expected. In this respect, it is interesting to note that nonlinear kinetics in the course of phase transfer catalytic reaction were observed in 1973 by Starks and Owens [31] during the biphasic cyanide displacement on 1-halooctanes. Other liquid-liquid biphasic experiments exhibiting autocatalytic behavior have been described by Rathman et al. [32]—for instance, the synthesis of *N*,*N*-dimethyldodecylamine *N*-oxide from *N*,*N*-dimethyldodecylamine and hydrogen peroxide or the synthesis of alkylphenyl ethers from alkyl halides and phenates in two-phase systems—and by Walde et al. [33] during the formation of fatty acid vesicles from alkaline hydrolysis of octanoic and oleic anhydrides. The behavior of this last autocatalytic reaction is so striking that several authors have attempted a kinetic modeling approach. First, Mavelli and Luisi [34] assumed two interfacial reactions: a slow one at the macroscopic interface and a rapid one at the vesicle surface. Then Coveney and Wattis [35] gave a nonequilibrium macroscopic description of vesicles formation and self-replication. From a more general point of view, it can be concluded that the dynamics of all these reactions show induction periods very similar to those we have found for the biphasic alkaline hydrolysis of ethyl alkanoates. This may point out that a nonlinear phase transfer takes place in these systems as well.

Liquid-liquid biphasic reactions in which reaction products have an influence on the interfacial properties

appear to be a new class of nonlinear chemical systems. Kinetic bistability in a continuous stirred tank reactor (CSTR) during the biphasic alkaline hydrolysis of ethyl octanoate [36] appears to be the first experimental example of such highly nonlinear behavior. Further examples of systems in which autocatalytic behavior is expected can be found in classical organic chemistry, such as the sulfonation of aromatic compounds or acetalization of sugars.

REFERENCES

1. P. R. Kust and J. F. Rathman, Langmuir *11*:3007–3012 (1995).
2. P. A. Bachmann, P. L. Luisi, and J. Lang, Nature *357*: 57–59 (1992).
3. J. Billingham and P. V. Coveney, J. Chem. Soc. Faraday Trans. *90*:1953–1959 (1994).
4. Y. A. Chimadzhew, M. Maestro, and F. Mavelli, Chem. Phys. Lett. *226*:56–62 (1994).
5. M. Maestro, Mol. Eng. *6*:391–403 (1996).
6. P. V. Coveney, A. N. Emerton, and B. M. Boghosian, J. Am. Chem. Soc. *118*:10719–10724 (1996).
7. P. V. Coveney and J. A. D. Wattis, Proc. R. Soc. Lond. A *452*:2079–2102 (1996).
8. P. S. Raghavan and V. S. Srinivasan, Proc. Indian Acad. Sci. (Chem. Sci.) *98*:199–206 (1987).
9. (a) T. Buhse, R. Nagarajan, D. Lavabre, and J. C. Micheau, J. Phys. Chem. *101*:3910–3917 (1997); (b) T. Buhse, D. Lavabre, R. Nagarajan, and J. C. Micheau, J. Phys. Chem. *102*:10552–10559 (1998). (c) J. Tixier, V. Pimienta, T. Buhse, D. Lavabre, R. Nagarajan, and J.-C. Micheau, Colloids and Surfaces A: Physicochem. Eng. Aspects *167*:131–142 (2000).
10. H. Polat, M. Polat, and S. Chander, AIChE J. *45*:1866–1874 (1999).
11. (a) V. Srinivas, G. A. Rodley, K. Ravikumar, W. T. Robinson, M. M. Turnbull, and D. Balasubramanian, Langmuir *13*:3235–3239 (1997); (b) V. Srinivas and D. Balasubramanian, Langmuir *14*:6658–6661 (1998).
12. M. M. Sharma and A. K. Nanda, Trans. Inst. Chem. Eng. *46*:T44–T52 (1968).
13. A. J. Engel and O. A. Hougen, AIChE J. *9*:724–729 (1963).
14. (a) D. P. Evans, J. J. Gordon, and H. B. Watson, J. Chem. Soc. 1439–1444 (1938); (b) G. Davies and D. P. Evans, J. Chem. Soc. 339–345 (1940).
15. (a) F. M. Menger and C. E. Portnoy. J. Am. Chem. Soc. *89*:4698 (1967); J. Am. Chem. Soc. *90*:1875 (1968); (b) J. H. Fendler and E. J. Fendler, *Catalysis in Micellar and Macromolecular Systems*, Academic Press, New York, 1975.
16. R. Becker and W. Döring, Ann. Phys. *24*:719 (1935).
17. E. A. G. Aniansson, S. N. Wall, M. Almgren, H. Hoffmann, I. Kielmann, W. Ulbricht, R. Zana, J. Lang, and C. Tondre, J. Phys. Chem. *80*:905–922 (1976).
18. I. Danielsson and P. Stenius, J. Colloid Interface Sci. *37*:264–280 (1971).
19. P. Mukerjee, J. R. Cardinal, and N. R. Desai, in *Micellization, Solubilization, and Microemulsions* (K. L. Mittal, ed.), Plenum, New York, 1977, p. 241.
20. R. Nagarajan, M. A. Chaiko, and E. Ruckenstein, J. Phys. Chem. *88*:2916–2922 (1984).
21. (a) M. Aamodt, M. Landgren, and B. Jönsson, J. Phys. Chem. *96*:945–950 (1992); (b) M. Landgren, M. Aamodt, and B. Jönsson, J. Phys. Chem. *96*:950–961 (1992).
22. S. Karaborni, N. M. van Os, K. Esselink, and P. A. J. Hilbers, Langmuir *9*:1175–1178 (1993).
23. P. Plucinski and W. Nitsch, J. Phys. Chem. *97*:8983–8988 (1993).
24. M. Hebrant and C. Tondre, Anal. Sci. *14*:109–115 (1998).
25. J. Otsuki and M. Seno, J. Phys. Chem. *95*:5234–5238 (1991).
26. L. Benjamin, J. Phys. Chem. *68*:3575–3581 (1964).
27. M. H. Abraham, J. Chem. Soc. Faraday Trans. 1 *80*: 153–181 (1984).
28. C. Tanford, *The Hydrophobic Effect*, Wiley, New York, 1973.
29. R. Nagarajan and E. Ruckenstein, Self-assembled systems, in *Equation of State for Fluids and Fluid Mixtures* (J. V. Sengers, ed.), Elsevier, Amsterdam, in press.
30. R. Nagarajan and E. Ruckenstein, Langmuir *7*:2934–2969 (1991).
31. C. M. Starks and R. M. Owens, J. Am. Chem. Soc. *95*: 3613–3617 (1973).
32. C. Siswanto, T. Battal, O. E. Schuss, and J. F. Rathman, Langmuir *13*:6047–6052 (1997).
33. P. Walde, J. Wick, M. Fresta, A. R. Mangone, and P. L. Luisi, J. Am. Chem. Soc. *116*:11649–11654 (1994).
34. F. Mavelli and P. L. Luisi, J. Phys. Chem. *100*:16600–16607 (1996).
35. P. V. Coveney and J. A. D. Wattis, J. Chem. Soc. Faraday Trans. *94*:233–246 (1998).
36. T. Buhse, V. Pimienta, D. Lavabre, and J. C. Micheau, J. Phys. Chem. A *101*:5215–5217 (1997).